Electron Bernstein wave emission from an overdense reversed field pinch plasma

P. K. Chattopadhyay, J. K. Anderson, T. M. Biewer, D. Craig, and C. B. Forest[a)]
Department of Physics, University of Wisconsin, Madison, Wisconsin 53706

R. W. Harvey
CompX, Del Mar, California 92014

A. P. Smirnov
Moscow State University, Moscow, Russia

(Received 11 October 2001; accepted 20 November 2001)

Blackbody levels of emission in the electron cyclotron range of frequencies have been observed from an overdense ($\omega_{pe}\sim 3\omega_{ce}$) Madison Symmetric Torus [Dexter *et al.*, Fusion Technol. **19**, 131 (1991)] reversed field pinch plasma, a result of electrostatic electron Bernstein waves emitted from the core and mode converted into electromagnetic waves at the extreme plasma edge. Comparison of the measured radiation temperature with profiles measured by Thomson scattering indicates that the mode conversion efficiency can be as high as $\sim 75\%$. Emission is preferentially in the X-mode polarization, and is strongly dependent upon the density and magnetic field profiles at the mode conversion point. © *2002 American Institute of Physics.* [DOI: 10.1063/1.1447253]

Electromagnetic waves in the electron cyclotron range of frequencies (ECRF) do not propagate in plasma confinement devices such as the reversed field pinch (RFP) and spherical tokamak (ST) because the plasmas are overdense ($\omega_{pe} \gg \omega_{ce}$, where $\omega_{pe}^2 = e^2 n_e/\varepsilon_0 m_e$ is the plasma frequency and $\omega_{ce} = eB/m_e$ is the cyclotron frequency). However, the electrostatic electron Bernstein wave (EBW) does propagate. It has been previously proposed and theoretically shown that EBWs may be suitable for driving current and heating in RFPs and STs[1,2] provided a technique for coupling to the waves can be found. Both fusion concepts would benefit from the localizable, efficient current drive predicted from the theory.

Two scenarios have been proposed for coupling electromagnetic waves to the EBW at the plasma edge. The first proposed (OXB) was a double mode conversion scenario in which an obliquely launched O-mode transforms to the slow branch of the X-mode which then mode converts into an EBW at the upper-hybrid resonance (UHR) in the plasma.[3,4] This scenario has been tested experimentally in the Wendelstein-7 (W7-AS) stellarator where both heating and emission have been observed in the ECRF in overdense plasmas.[5,6] The second scenario (XB) involves tunneling of a perpendicularly launched fast X-mode through a cutoff region at the plasma edge to the slow branch of the X-mode where it then mode converts to the EBW when the wave frequency equals the local upper hybrid frequency $\omega_{uh}^2 = \omega_{pe}^2 + \omega_{ce}^2$. The XB conversion has been alluded to theoretically[7] and it has been identified in a linear plasma device[8] and in ST.[9] Recently the XB process has been examined in detail and compared to the OXB scenario.[10] It was found that XB can be an efficient mode conversion process if the frequency is chosen to match conditions depending upon the details of the edge density profile. Neither radiation emitted through the XB mode conversion process nor heating via the launched wave has been observed.

In this Letter, we present the observations of electron cyclotron emission from a RFP. We speculate that the observed black body emission is generated in the EBW mode in the core of the plasma, propagates to the edge and is mode converted to the electromagnetic waves which are detected by an absolutely calibrated radiometer. The present experiment is the first observation of emission from an overdense plasma in the X-mode polarization and suggests that the XB process is responsible for the observed emission. By reciprocity, the measurements establish the viability of EBW heating in over-dense plasmas.

The theoretical model of the mode conversion efficiency for XB as presented in Ref. 10 provides a context for understanding the observed emission levels. The maximum XB mode-conversion efficiency is predicted to be

$$C_{\max} = 4e^{-\pi\eta}(1-e^{-\pi\eta}), \tag{1}$$

where

$$\eta = \frac{1}{\alpha}\left[\frac{\omega_{ce}L_n}{c}\right]_{\mathrm{UHR}} [\sqrt{1+\alpha^2}-1]^{1/2} \tag{2}$$

and $\alpha = (\omega_{pe}/\omega_{ce})$ and $L_n = n/|\partial n/\partial r|$ is the density scale length. All quantities are to be evaluated at the UHR layer where the mode conversion process takes place. In the Madison Symmetric Torus (MST), the UHR associated with frequencies $\omega_{ce} < \omega < 2\omega_{ce}$ is near the extreme edge of the plasma as seen in Fig. 1. The mode conversion efficiency is therefore predicted to be a strong function of the density profile shape. It also depends upon the magnetic field profile through the parameters α and ω_{ce}. Physically, η is related to

a)Electronic mail: cbforest@facstaff.wisc.edu

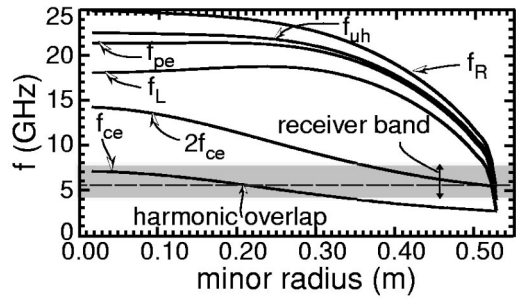

FIG. 1. Cutoff and resonance frequencies in ECRF for $I_P=250$ kA, n_e (central) $=6\times10^{18}$ m^{-3} MST plasmas. The equilibrium is a solution of the Grad–Shafranov equation fit to the available magnetic data.

the distances between the right hand cutoff, left hand cutoff layers, and the upper hybrid resonance normalized to the vacuum wavelength of the radiation. Transmission occurs when the waves reflected from the left hand cutoff and right hand cutoff layers destructively interfere.

The experiments described in this Letter were performed in the MST[11] reversed field pinch [major radius $(R)=1.5$ m, minor radius $(a)=0.52$ m]. Unlike tokamaks and stellarators, the RFP has a magnetic field which is proportional to the plasma current and whose magnitude depends primarily upon minor radius rather than major radius. The magnetic field increases by approximately a factor of 2 from the edge to the core. Typical profiles of cutoffs and resonances in the MST are shown in Fig. 1. Surfaces of constant $|B|$ are nearly aligned with the magnetic flux surfaces as seen in Fig. 2.

The projection of a three dimensional ray trajectory onto a poloidal plane is also shown in Fig. 2. This 5.5 GHz ray launched from the outside of the torus (using the GENERAY ray tracing techniques described in Ref. 1) at a poloidal position of 19° above the outer midplane (location of antenna during experiment). By reciprocity, emission recieved by the antenna must occur along the same ray trajectory for a wave propagating outward. The computed parallel component of the refractive index $N_\parallel$ along the ray indicate that the EBW emission will occur at a position along the trajectory where $N_\parallel\sim2$, and that the ray undergoes a $N_\parallel$ downshift into the antenna pattern of the receiving antenna as it propagates outward. The absorption calculations indicate that the plasma is optically thick [optical depth $(\tau)\gg10$] such that the plasma will emit as a blackbody, and that the Doppler shift leads to emission from a location several cm to the low field side of the cold electron cyclotron (EC) resonance location (Fig. 2).

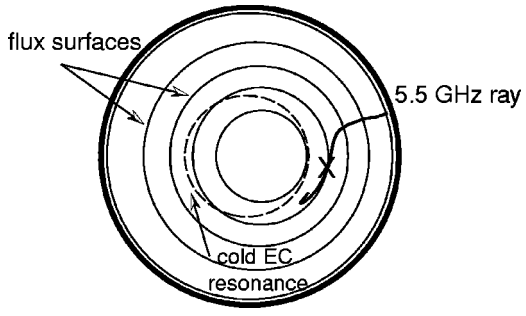

FIG. 2. Poloidal flux and a constant $|B|$ (resonance for 5.5 GHz) surface. The 2D equilibrium is a solution of the Grad–Shafranov equation fit to the available magnetic data. The position along the ray where the optical thickness is 1 is labeled $(\times)$ to indicate the location of the source of observed emission.

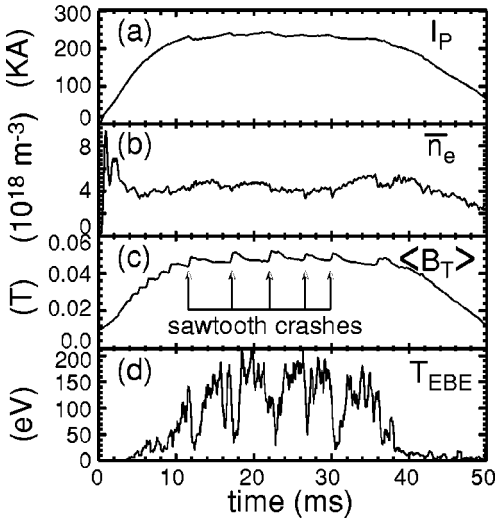

FIG. 3. Time histories of the plasma current (I_P), line averaged plasma density $(\overline{n_e})$, average toroidal magnetic field and radiation temperature of EBE at 5.75 GHz.

Emission was measured by a broadband double-ridge horn antenna (aperture 5 cm$\times$5 cm), with an antenna gain of 13–17 dB ($\Delta N_\parallel=\pm0.34-\pm0.22$) over the bandwidth 3.8–8.2 GHz. The antenna is movable radially and located 19° above the toroidal midplane. For these experiments the antenna was located in a 4.5 in. port 5 cm behind the inner wall of the vacuum vessel and ≈7 cm from the location of the upper hybrid resonance. The antenna views the plasma radially (perpendicular to $\mathbf{B}$ with $N_\parallel=0$) and is rotatable to receive radiation with $\mathbf{E}_{\mathrm{rad}}\|\mathbf{B}$ or $\mathbf{E}_{\mathrm{rad}}\perp\mathbf{B}$ corresponding to O-mode and X-mode emission from the plasma edge. The emission was detected by a 16 channel homodyne radiometer. Two ultra-low noise rf amplifiers provide 80 dB of gain; a power splitter separates the power into 16 bandpass filters (125 MHz bandwidth each) and diode detectors. The radiometer has a low noise temperature (1600 K to 2500 K within the 4–8 GHz range) since no local oscillator was used. The radiometer was absolutely calibrated with thermal emission from microwave absorption material (eccosorb) at liquid nitrogen (77 K) and room temperature (300 K).

Figure 3 shows time histories of the plasma current, plasma density, average magnetic field for a $I_p=250$ kA. The radiometer signal in Fig. 3(d) corresponds to the frequency $f=5.75$ GHz, corresponding to emission from the core. The line average electron density is $\overline{n_e}\sim4\times10^{18}$ m^{-3}. The plasmas are clearly overdense and do not support propagating electromagnetic waves. Emission drops dramatically at ''sawteeth,'' flux generation events which sustain the poloidal current in the edge of the RFP.[12] The MHD activity during a sawtooth is global and affects all observable equilibrium quantities in a reproducible fashion. In particular, the sawtooth crashes strongly influence the

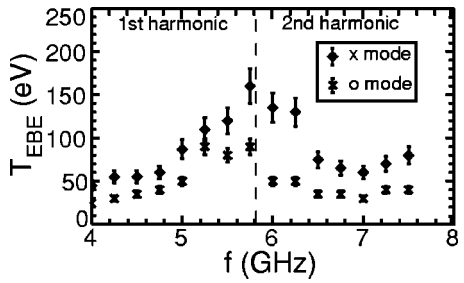

FIG. 4. Measured O- and X-mode radiation temperature vs frequency. The vertical dashed line at 5.8 GHz separates two cyclotron harmonics.

edge density profile and hence the mode conversion efficiencies.

The observed spectra for both O ($\mathbf{E}_{rad}\|\mathbf{B}$) and X mode ($\mathbf{E}_{rad}\perp\mathbf{B}$) are shown in Fig. 4. These spectra represent an ensemble average of approximately 25 sawteeth during the period between sawtooth crashes. The radiation temperatures for both polarizations are comparable to the electron temperature as measured by Thomson scattering and is therefore of blackbody levels. However, the X-mode polarization has a measurably higher radiation temperature. The plotted uncertainty represents both the statistical variation associated with the inherent fluctuation levels and the systematic error associated with calibration. The difference between the radiation temperatures for the two polarizations is attributable to the differences in the mode conversion efficiencies from EBW to O-mode and X-mode, the dependence of the mode conversion efficiencies on angle, and the antenna pattern. The viewing geometry used in these experiments was not optimized for coupling to the O-mode. The antenna recieves only linear polarization while the polarization of the X- and O-modes become elliptical for oblique propagation. We have calculated the polarization for obliquely propagatting O-mode using cold plasma wave equation using our experimental parameters. It was found that for obliquely propagating O-mode the power in X-mode polarization ($\mathbf{E}_{rad}\perp\mathbf{B}$) is less than 10% of the power in O-mode polarization ($\mathbf{E}_{rad}\|\mathbf{B}$). Also the emission for $\mathbf{E}_{rad}\perp\mathbf{B}$ was measured to be larger than for $\mathbf{E}_{rad}\|\mathbf{B}$ from which we conclude that radiation received with $\mathbf{E}_{rad}\perp\mathbf{B}$ is primarily coming from X-mode.

Figure 5 shows the radiation temperature measured by the radiometer (T_{EBE}) mapped to plasma radius (r). Ray tracing calculations are used to determine the emission location and include the Doppler shift from the cold EC resonance as described in Ref. 1. By comparing the temperature as measured by Thomson scattering ($T_{Thomson}$) with T_{EBE} the mode-conversion efficiency can be inferred from the ratio $T_{EBE}/T_{Thomson}$ at a given position/frequency. For example, at $f=4.0$ GHz which corresponds to $r=37$ cm, $T_{EBE}/T_{Thomson}\approx 0.4$. The mode conversion efficiency appears to increase with frequency. For frequencies higher than 5.75 GHz, harmonic overlap occurs (with caveats mentioned below); core emission from the fundamental resonance is absorbed at the second harmonic near the edge. The observed levels of emission are consistent with emission from the second harmonic at the edge.

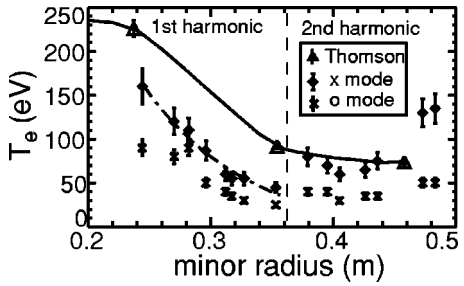

FIG. 5. Spectrum for O- and X-mode EBE radiation temperature mapped to minor radius. Also shown is the electron temperature measurements from Thomson scattering. The vertical dashed line separates two cyclotron harmonics.

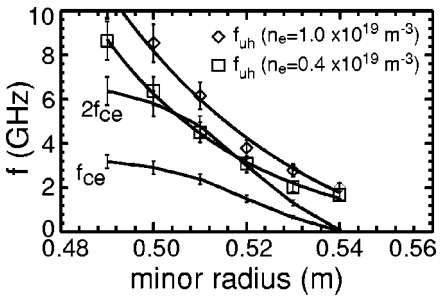

FIG. 6. Edge profiles for cyclotron and upper hybrid frequencies for $\overline{n_e}=0.4\times10^{19}$ m^{-3} and 1.0×10^{19} m^{-3}. These frequencies include the porthole perturbation to the equilibrium magnetic field, unlike Fig. 1.

To investigate the effect of edge density profiles on mode conversion efficiency, discharges of different line average densities were compared. The edge density profile was measured with a triple Langmuir probe on a shot to shot basis over a large number of similar discharges for two line average densities namely $\overline{n_e}=0.4\times10^{19}$ m^{-3} and 1.0×10^{19} m^{-3}. Edge magnetic fields and hence cyclotron frequencies were calculated based on known behavior of the magnetic field in the edge near a porthole. On MST, the vacuum vessel at 0.52 m serves as both a toroidal field magnet and as a flux conserver; the magnetic field at the edge of the MST is primarily poloidal and drops off quickly through the porthole over a scale length of the order of radius of the prothole. Diagnostic portholes interupt the image currents in the vessel wall, which in turn affects the cyclotron frequency in vicinity of the antenna.

Figure 6 shows profiles of the first and second harmonic cyclotron frequencies and the upper hybrid frequency calculated from the density and magnetic field profiles. From measured edge n_e profiles, the density gradient scale lengths at the UHR are estimated to be $L_n\sim1.4$ cm for both low and high line average density. However, for a given frequency, the location of UHR surface shifts outward for higher density. When the UHR surface is between f_{ce} and $2f_{ce}$ (i.e., the low density case) blackbody emission associated with the core is observed. However, when the density is high and $f_{uh}>2f_{ce}$ harmonic overlap occurs and the edge temperature is seen. This overlap criterion restricted the observation of radiation from the interior of the plasma at low densities. Indeed, for densities above 1.0×10^{19} m^{-3} the entire observed spectrum dropped to levels comparable to the electron temperature at the plasma edge.[13] The evidence for the role

of the edge density gradient on coupling efficiency is inferred from fluctuations. There is a strong correlation between the density fluctuations in the immediate vicinity of the antenna and the fluctuations in T_{EBE}.

It should be noted that the role of wall reflections is not expected to be large in MST since the antenna has high gain and close to the plasma. Also, the emitting layer is optically thick. The mode-conversion efficiency, as measured from the emission level compared to Thomson scattering measurements, can be compared to the theoretical value in Eq. (1). Significant uncertainties in the interpolation of the Thomson measurements and estimates of $(L_n)_{\mathrm{UHR}}$ and α from the Langmuir probe measurements make a precise determination of η difficult. But near harmonic overlap (at $\sim$5.75 GHz) the value of α (~ 2) is well defined. In MST, for line average electron density $\overline{n_e} \sim 4\times 10^{18}$ m^{-3}, the density scale length $(L_n)_{\mathrm{UHR}} \sim 1.4$ cm, $\alpha = 2$ for 5.75 GHz giving $\eta = 0.46$. The theoretical maximum mode conversion efficiency $C_{\max} \sim 70\%$, experimentally we find the efficiency is 75%. However, to find mode conversion efficiency at all frequency and hence to estimate the temperature a precise spacial measurement of electron density and magnetic field field at edge are necessary. This might put a hindrance to the use of EBE as a standard diagnostic tool for temperature measurement. Nonetheless, our observation shows that XB mode conversion is efficient for suitable edge conditions which indicates the possibilities of heating and current drive in overdense plasmas with EBW.

In summary, electron-cyclotron radiation from an overdense plasma has been observed with both X- and O-mode polarization. Emission of BX has been observed for the first time. The radiation temperature when compared to temperature measured by Thomson scattering can be used to estimate the mode conversion efficiency. The necessity of exact knowledge of L_n and phase factor makes it difficult to use EBE as a standard diagnostic for electron temperature. The BX mode conversion efficiency is observed to be as high as 75% for low density discharges. By reciprocity, the observation of emission shows that heating and current drive in overdense plasmas such as RFPs and STs may be feasible by perpendicularly launched X-mode power in the ECRF, provided the density profiles are suitable.

ACKNOWLEDGMENT

This work was supported by the U.S. Department of Energy.

[1] C. B. Forest, P. K. Chattopadhyay, R. W. Harvey, and A. P. Smirnov, Phys. Plasmas **7**, 1352 (2000).
[2] C. B. Forest, M. Ono and G. Greene, Bull. Am. Phys. Soc. **35**, 2057 (1990).
[3] J. Preinhaelter and V. Kopecký, J. Plasma Phys. **10**, 1 (1973).
[4] H. Weitzner and D. B. Batchelor, Phys. Fluids **22**, 1355 (1979).
[5] H. P. Laqua, V. Erckmann, and H. J. Hartfuß, Phys. Rev. Lett. **78**, 3467 (1997).
[6] H. P. Laqua, H. J. Hartfuß, and W7-AS Team, Phys. Rev. Lett. **81**, 2060 (1998).
[7] S. Nakajima and H. Abe, Phys. Rev. A **38**, 4373 (1988).
[8] H. Sugai, Phys. Rev. Lett. **47**, 1899 (1981).
[9] G. Taylor, P. Efthimin, B. Jones, T. Munsat, J. Spaleta, J. Hosea, R. Kaita, R. Majeski, and J. Menard, Rev. Sci. Instrum. **72**, 285 (2001).
[10] A. K. Ram and S. D. Schultz, Phys. Plasmas **7**, 4084 (2000).
[11] R. N. Dexter, D. W. Kerst, T. W. Lovell, S. C. Prager, and J. C. Sprott, Fusion Technol. **19**, 131 (1991).
[12] S. Hokin, A. Almagri, S. Assadi, J. Beckstead, G. Chartas, N. Crocker, and M. Cudzinovic, Phys. Fluids B **3**, 2241 (1991).
[13] The observant reader will note that the first two points of second harmonic EBE are unexpectedly high for low density case. This, again, is likely due to the local density and magnetic field in the 4.5 in. antenna port having $f_{UH} < 2\, f_{ce}$ where the frequencies are equal to f_{uh} allowing the core emission to propagate to the edge.